Block of Neuronal Chloride Channels by Tetraethylammonium Ion Derivatives

DOROTHEA Y. SANCHEZ and ANDREW L. BLATZ

From the Department of Physiology, University of Texas Southwestern Medical Center, Dallas, Texas 75235

ABSTRACT The block by the symmetric tetraethylammonium (TEA) ion derivatives tetrapropylammonium (TPrA), tetrabutylammonium (TBA), and tetrapentylammonium (TPeA) ions of fast chloride channels in acutely dissociated rat cortical neurons was studied with the excised inside-out configuration of the patch-clamp technique. When applied to the intracellular membrane surface, all three of the quaternary ammonium compounds (QAs) induced the appearance of short-lived closed states in a manner consistent with a blocking mechanism where the blocker preferentially binds to the open kinetic state and completely blocks ion current through the channel. The drug must leave the channel before the channel can return to a closed state. The mechanism of block was studied using one-dimensional dwell-time analysis. Kinetic models were fit to distributions of open and closed interval durations using the Q-matrix approach. The blocking rate constants for all three of the QAs were similar with values of $\sim 12-20 \times 10^6$ $M^{-1}s^{-1}$. The unblocking rates were dependent on the size or hydrophobicity of the QA with the smallest derivative, TPrA, inducing a blocked state with a mean lifetime of ~ 90 μs, while the most hydrophobic derivative, TPeA, induced a blocked state with a mean lifetime of ~ 1 ms. Thus, it appears as though quaternary ammonium ion block of these chloride channels is nearly identical to the block of many potassium channels by these compounds. This suggests that there must be structural similarities in the conduction pathway between anion and cation permeable channels.

INTRODUCTION

Most potassium channels are blocked to some extent by tetraethylammonium ion and its more hydrophobic derivatives (Stanfield, 1983; Hille, 1992). Many K channels contain two discrete types of TEA blocking sites, an internal site located within the electric field of the membrane that has a high affinity for hydrophobic quaternary ammonium ions, and an external site that is more superficially located and that exhibits only weak binding for hydrophobic TEA derivatives (Armstrong, 1975). Early work on TEA block of the delayed rectifier K channel of squid axon

Address correspondence to Dorothea Y. Sanchez, Department of Biology, Astra Arcus USA, P.O. Box 20890, Rochester, NY 14602.

Dr. Blatz's current address is Axon Instruments, Inc., 1101 Chess Drive, Foster City, CA 94404.

J. GEN. PHYSIOL. © The Rockefeller University Press · 0022-1295/95/11/1031/16 $2.00
Volume 106 November 1995 1031–1046

led to a model for the structure of these channels that, with small modifications, is still used today to describe almost all ion channel permeation pathways. Most modern studies of K channels using powerful molecular biological approaches continue to use TEA and its derivatives both as assays for specific channel activity, and as probes for the channel's internal structure (for example see MacKinnon and Yellen, 1990; Yellen, Jurman, Abramson, and MacKinnon, 1991; Hartman, Kirsch, Drew, Taglialatela, Joho, and Brown, 1991; Choi, Mossman, Aube, and Yellen, 1993). In more broad applications, TEA and its derivatives are widely used to differentiate processes dependent on K channels from those dependent on other kinds of ion channels.

We have recently reported the TEA, applied either from the extracellular or intracellular membrane surface of excised patches, blocks the neuronal fast Cl channel in a manner that is identical to the block of K channels (Sanchez and Blatz, 1992, 1994). The block appears as a reduction in the single-channel current amplitude.

In the present study, we show that more hydrophobic derivatives of TEA block the fast Cl channel and that individual blocking events are resolvable. Dwell-time histograms were compiled to determine the number of kinetic states for the Cl channel. Block of the channel, if resolvable, would appear as a novel kinetic closed state in the dwell-time distribution. If the open dwell-time distribution is affected, this suggests the compound binds the open state of the Cl channel. Reaction scheme simulations were performed to determine the most likely kinetic scheme and the rate constants between states.

METHODS

The experimental methods for recording currents from single fast Cl channels have been described elsewhere in detail (Blatz and Magleby, 1986*a*,*b*; Blatz, 1991; Sanchez and Blatz, 1992, 1994), and will only briefly be described here.

Rat Cortical Neuron Isolation

Rat cortical neurons were isolated from slices of young (4-15-d-old) rat brains using the method of Kay and Wong (1986). Plugs of frontal and parietal cortical tissue ~500 μm thick and 1 mm in diameter were incubated in Pipes saline (solution compositions below) containing trypsin (0.65 mg/ml, Sigma Type III; Sigma Chemical Company, St. Louis, MO) for 0.5-1.0 h at 37°C). After trypsin digestion, the cortical plugs were washed four times at room temperature with Pipes saline. When needed, 1–3 plugs were dissociated into single cell suspensions by trituration through a fire-polished Pasteur pipette. Neurons were identified by their characteristic morphologies and were used within 1 h of dissociation.

Single-Channel Recording

Currents through single fast Cl channels were recorded from excised, inside-out membrane patches using the patch-clamp technique (Hamill, Marty, Neher, Sakman, and Sigworth, 1981). Data was collected from patches with only one active channel, i.e., patches lacking a second conductance level in their amplitude histogram. Single-channel currents were recorded with Axopatch 1B and 200A amplifiers and stored on FM tape (30 ips, Racal Store 4DS) (Axon Instruments, Inc., Foster City, CA). The current record was played, at reduced tape speed, into a micro-

computer with a 14-bit analogue-to-digital converter (Instrutech model VR10A) for off-line analysis. Except where noted, all currents were digitized at an effective sampling interval of 2.865 μs (actual sampling frequency of ~95 kHz and tape slowed by a factor of four). The effective filtering frequency was 15 kHz. All experiments were carried out at room temperature (20–23°C).

Solutions

The composition (in millimolar) of the solutions used in these experiments were: Pipes saline: 120 NaCl, 5 KCl, 1 $CaCl_2$, 1 $MgCl_2$, 25 glucose, 20 Pipes (piperazine-*N*-*N*-bis-(2-ethanesulfonic acid), pH 7.0.

Tetrapropylammonium (TPrA), tetrabutylammonium (TBA), tetrapentylammonium (TPeA), and tetrahexylammonium (THA) compounds were obtained from Sigma Chemical Co. (Cl salts) and Fluka Chemical Corp. (Br salts; Ronkonkoma, NY). Solutions bathing the formerly intracellular surface of the membrane patch were conveniently switched by placing the tip of the electrode containing the patch into a microchamber (Barrett, Magleby, and Pallotta, 1982) connected to an eight-way valve and eight solution reservoirs.

Measurements of Single-Channel Amplitudes and Amplitude Distributions

For amplitude measurements the filtered, digitized raw current record was displayed on a video monitor and horizontal cursors were adjusted by eye to the fully closed and open channel current levels. Additionally, amplitude distributions were collected and the closed and open current amplitudes were determined from these. Amplitude distributions were collected from the filtered, digitized current record by binning individual points according to their amplitudes. Usually only those sweeps of 640 points that contained at least one open event were used to construct amplitude distributions. Approximately 1 min of data was included in each amplitude histogram. Usually every eighth sampled point was used for amplitude distributions that would be equivalent to an effective sampling interval of 21.18 μs.

Measurement of Durations of Open and Closed Intervals

A 50% threshold method was used to determine the durations of open and closed intervals from the digitized current data. The current records were monitored visually during playback into the computer to prevent the inclusion of noise spikes and patch breakup events. Once digitized, the data were again examined, both visually, and using stability plots (see below), to insure that baseline shifts, noise artifacts, and shifts in gating kinetics (moding) were not present in the portions of the experimental record used for analysis. At the 378-kHz sampling rate (1 point/2.648 μs) used in these experiments the sampling errors described by McManus, Blatz, and Magleby (1987) were negligible.

Stability plots (Blatz and Magleby, 1986*b*; Weiss and Magleby, 1990; Blatz, 1991) were constructed and examined for all interval duration data sets by calculating the mean open duration over subsets (usually containing 50–200 events) of the data record and plotting this as the running mean open or closed interval duration vs interval number. Periods of nonnormal kinetic activity such as the buzz mode or the subconductance mode (Blatz and Magleby, 1986*b*; Blatz, 1991) were excluded from subsequent analysis.

The number of exponential components required to fit the distributions of open and closed dwell-times was determined using the likelihood ratio test (Rao, 1973; Horn and Lange, 1983). Starting with one exponential component, the number of components fitted to the data was increased, one at a time, until the improvement of fit was no longer significant ($P < 0.05$). The most likely number of exponential components was the highest number that gave a statistically significant improvement of the fit.

Fitting Kinetic Models to Single-Channel Data in the Presence of Blockers

Methods described by Colquhoun and Sigworth (1983), Blatz and Magleby (1986*a,b*), McManus and Magleby (1991), and Weiss and Magleby (1990) were used to fit kinetic reaction schemes to the distributions of open, closed, and blocked single-channel interval durations in the absence and presence of QAs. The Q-matrix approach of Colquhoun and Hawkes (1983), with the appropriate correction for missed events (Blatz and Magleby, 1986*a*), was used in an iterative fashion to determine the most likely parameter values.

RESULTS

Neuronal Fast Cl Channel Currents in the Presence of QAs

Representative single-channel currents recorded from the same neuronal fast Cl channel under control conditions and in the presence of 500 μM TPrA, TBA, or TPeA are shown in Fig. 1. In the absence of drug, fast Cl channels exhibited characteristic bursts of short-duration open and closed events separated by closed events of longer durations. In this particular experiment, the mean open duration was 0.42 ms in the absence of QAs. In the presence of any of the three tested QAs the bursts were characterized by a drastic increase in the number of short (~0−300 μs), but apparently complete, closed events resulting in a much noisier appearance. The duration of the bursts also appeared to increase in the presence of QAs. The simplest interpretation of these observations is that the larger QAs bind to the open channel and completely block all current flowing through neuronal fast Cl channels with a mean blocked lifetime on the order of 100's of microseconds. Burst duration is increased because the QA must unbind for the channel to proceed to a normal closed state. The measured mean open durations in the presence of TPrA , TBA, and TPeA were (in milliseconds): 0.24, 0.21, 0.20, respectively, in this experiment. These observations are different from the effects of block by the smaller QA, TEA, which appeared as a reduction in single-channel current amplitude with little change in single-channel kinetic activity.

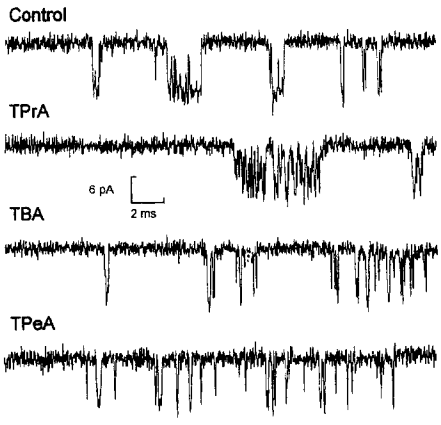

FIGURE 1. Selected single-channels currents from neuronal fast Cl channels under control conditions and in the presence of 1 mM of TPrA, TBA, and TPeA. Currents were recorded onto FM tape with no additional filtering (measuring bandwidth of 15 kHz). Currents were digitized at 2.486 μs/point, converted to ASCII text files and displayed using SigmaPlot for Windows (Jandel Scientific, Corte Madora, CA). Holding membrane voltage of −47 mV, $[KCl]_i$: 1 M, $[KCl]4_o$: 140 mM.

QAs Decrease Mean Open Lifetimes

The histogram in Fig. 2 presents the effects on mean open duration of the three different QAs for three different experiments. Although the histogram in Fig. 2 gives the impression of a correlation between QA size and a reduction in the mean open duration, there were no significant differences among the mean open durations obtained in the presence of any of the QAs. The control value was significantly larger than the values obtained in the presence of the QAs considered separately or combined.

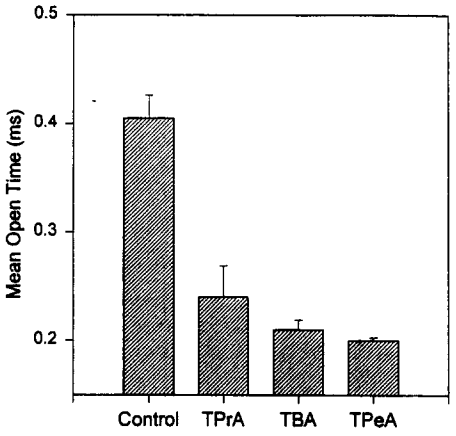

FIGURE 2. Dependence of mean open duration on presence of three QAs. Mean values and standard errors calculated from three different membrane patches. All three QA conditions were significantly different from control (Student's *t* test), but QAs were not significantly different from one another. Conditions as in Fig. 1.

The QA-Blocked State Is Completely Closed

All-points amplitude distributions were obtained from one minute of activity from the channel in Fig. 1 and are presented in Fig. 3. The distributions were aligned such that the peaks representing the current amplitude of the closed channel current were superimposed at 0 pA. The amplitudes of the peaks representing the open channel current were all about equal (13.0, 12.8, 13.0, and 12.4 pA for control, TPrA, TBA, and TPeA, respectively, in this experiment) confirming that in the presence of larger QAs the channel current fluctuated between a fully open and a fully closed (or blocked) conductance state. No evidence of partially blocked currents was apparent from the raw current records or from any of the amplitude distributions.

QAs Preferentially Block Open States

The decreased mean open dwell time observed in the presence of QAs suggested that these compounds preferentially block the open kinetic state or states. A more detailed analysis is presented below where the open and closed dwell-time distributions from one patch in the presence of 100, 500, and 1,000 TPrA are examined.

Single neuronal fast Cl channel currents in the presence of increasing concentrations of internal TPrA are shown in Fig. 4. These selected current traces, recorded

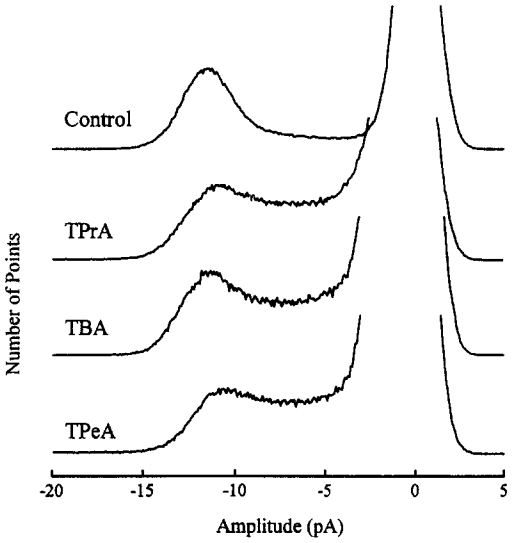

FIGURE 3. All-points amplitude distributions calculated from 1 min of single-channel activity from the patch shown in Fig. 1. The peaks closest to zero current were aligned at 0 pA and the Y-axis was scaled individually such that the peaks representing the open channel current level were approximately the same height. Conditions as in Fig. 1.

at 15 kHz, demonstrate that the major effect of TPrA block (at concentrations from 100 to 1,000 μM) was an increase in the frequency of short closed events and a decrease in the mean open duration. The longer closed intervals seemed to be relatively unaffected by up to 5 mM TPrA. However, at 5 mM TPrA there was an apparent reduction of the magnitude of the open channel current, presumably due to filtering of very brief open events. Because of this, only data collected at concentrations of 1 mM or less were used for subsequent analysis.

Dwell-Time Distributions Indicate a New Closed State and a Shorter Mean Open Time with TPrA

Distributions of open and closed interval durations recorded from the same channel as in Fig. 4 in the presence of increasing concentrations of TPrA are presented in Figs. 5 and 6. The number of exponential components required to fit these distributions was determined using the likelihood ratio test (Rao, 1973; Horn and

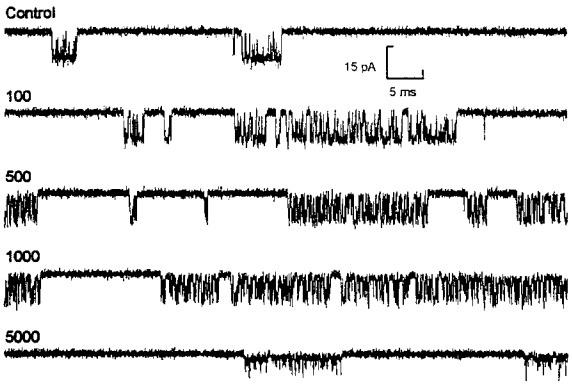

FIGURE 4. Selected single-channel currents from a membrane patch containing one fast Cl channel under control conditions and in the presence of 100, 500, 1,000, and 5,000 μM TPrA. Data recording and filtering conditions same as in Fig. 1.

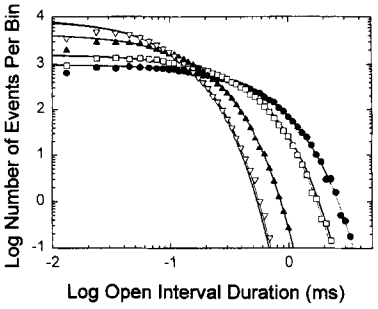

FIGURE 5. Open dwell-time distributions under control conditions (*filled circles*), and in the presence of TPrA (in micromolar): 100, *open squares*; 500, *filled triangles*; 1000, *open triangles* from channel whose currents were shown in Fig. 4. Thinner solid lines represent the most likely exponential time constants and areas as shown in Table I. Thicker solid lines represent the most likely set of rate constants for Scheme I with all rate constants freely variable.

Lange, 1983). Tables I and II present the time constants and areas from the exponential equations that best fit these open and closed interval dwell-time distributions. TPrA decreased the mean open time (τ) of the channel in a concentration dependent fashion (Fig. 5 and Table I). In addition, TPrA added a new component ($\sim$0.09 ms) to the distribution of closed dwell times. The area of this new component increased with increasing blocker concentration. Concomitant with this increase in area there is a decrease in the areas of all other closed kinetic states, except the first. The first state appears to increase in area, slightly. This is likely an artifact of filtering. This shifting of area to the blocked kinetic state with proportional decreases in the other closed states, together with the decrease in the time constant for the open state, indicates that the blocker binds the open state and does not affect any of the transitions between the other states.

The solid lines in Figs. 5 and 6 were calculated from the time constants and areas of Tables I and II. As expected by visual inspection of the raw current traces, the open time constant decreased with increasing TPrA concentration. The effect of internal TPrA on the closed interval durations was more complex. TPrA increased the number of exponential components required to adequately fit the closed distribution. The number of components was six in the control recording and increased

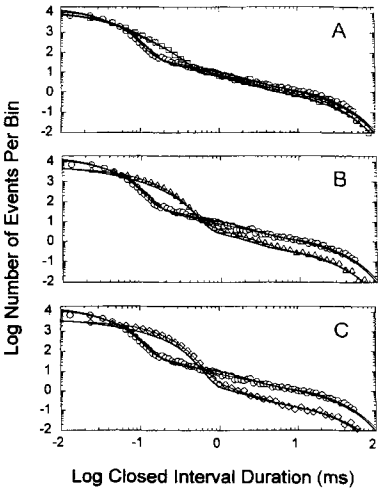

FIGURE 6. Closed dwell-time distributions under control (*open circles* in all three plots) and in the presence of TPrA (in micromolar): (*A*) 100, *squares*; (*B*) 500, *triangles*; (*C*) 1,000, *diamonds*. Thick and thin lines are as in Fig. 5.

TABLE I

Effects of TPrA on Distribution of Open Intervals

	[TPrA]$_i$ μM							
	0		100		500		1000	
n	τ	A	τ	A	τ	A	τ	A
1	0.38	1.0	0.23	1.0	0.10	1.0	0.06	1.0

Time constants (τ) in ms and fractional areas (A) represent the most likely parameters for the sums of exponential components that describe the distributions of all open interval durations in the presence of the indicated concentrations of intracellular TPrA. Bandwidth of 15 kHz. Membrane potential of −47 mV.

to seven in the presence of 100, 500, and 1,000 μM TPrA. Examination of the fitted values for the time constants and areas for the distribution of closed durations in Table II suggests that the exponential component with a time constant of 0.08 ms (100 μM TPrA) represents the blocked channel state. This is so because this component is the only one in which the relative area increases by an amount that would be required to account for the decrease observed in the mean open lifetime.

Blocking and Unblocking Rate Constants for TPrA

From the time constants in Tables I and II one can determine blocking and unblocking rate constants for TPrA. The time constant or mean lifetime of any one state equals the reciprocal of the sum of the rate constants leaving that state. Thus, the blocking rate constants at 100, 500, and 1,000 μM TPrA can be calculated to be 1.72, 7.37, and 14.0 ms^{-1}, respectively (Fig. 7) and the blocking reaction proceeds with first order kinetics. The first order rate constant for block is $\sim 13.6 \times 10^6$ M^{-1} s^{-1}. The unblocking rate constant is not significantly affected by blocker concentration (the % change is small relative to the change from control) and can be calculated

TABLE II

Effects of TPrA on Distributions of Closed Intervals

	[TPrA]$_i$ μM							
	0		100		500		1000	
n	τ	A	τ	A	τ	A	τ	A
1	0.02	0.88	0.03	0.55	0.03	0.14	0.06	0.056
2	0.23	0.03	0.080	0.35	0.090	0.808	0.111	0.909
3	1.38	0.03	0.46	0.021	0.301	0.019	0.380	0.016
4	9.62	0.02	1.79	0.024	1.44	0.017	1.64	0.007
5	21.20	0.04	13.27	0.032	11.74	0.011	13.31	0.006
6	94.78	0.0008	24.25	0.016	23.45	0.009	28.08	0.005
7	—	—	202.6	0.0001	140.6	0.002	241.1	0.00005

Time constants (τ) in ms and fractional areas (A) represent the most likely parameters for the sums of exponential components that describe the distributions of all closed interval durations in the presence of the indicated concentrations of intracellular TPrA. The ordering of components in this table is simply from shortest time constant to longest time constant, regardless of the number of components.

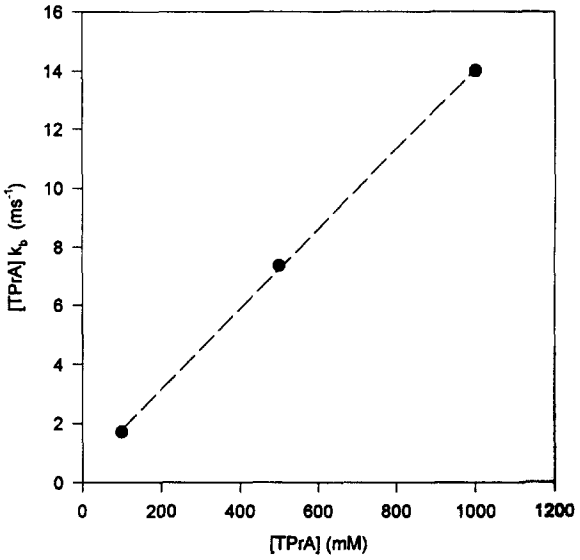

FIGURE 7. Rates for open to blocked transition at 100, 500, and 1,000 μM TPrA. Linear fit indicates first order kinetics. Slope of the line indicates blocking rate constant ($13.6 \times 10^6\ s^{-1}\ M^{-1}$).

to be ~11 ms^{-1}. All of the longer chain symmetric QAs appeared to block neuronal Cl channels in the same manner. We did not attempt to collect data for kinetic analysis for THA because of the uncertainty of its concentration due to its low solubility in aqueous solutions, although the effects of THA were qualitatively the same as those for the more soluble compounds. The results above were obtained from experiments with TPrA. Results for TBA were similar.

Q-Matrix Fitting to Obtain Rate Constants for TPrA Kinetic Scheme

Although determining the single correct kinetic model for the block of neuronal Cl channels by QAs is beyond the scope of this study, some sort of kinetic framework is required. To this end we have used maximum likelihood fitting techniques with the Q-matrix approach to determine most likely rate constants for simple kinetic reaction schemes. The distributions of closed interval durations of neuronal fast Cl channels exhibit at least five or six exponential components during normal activity, and therefore, a complete kinetic model for this channel must contain five or six closed kinetic states. The results of adjacent state analysis (McManus, Blatz, and Magleby, 1986; Blatz and Magleby, 1989) strongly argue for the presence of two open states for the fast chloride channel. In this study, the two open states were not resolvable due to filtering. However, the existence of rapidly interconverting open states would not complicate the interpretation of the relatively slow kinetics of QA block. Thus, as a framework for understanding the mechanism for TPrA block, the following Scheme was fit to the distribution of open and closed interval durations under control conditions and in the presence of 100, 500, and 1,000 μM TPrA:

$$C_8 \Leftrightarrow C_7 \Leftrightarrow C_6 \Leftrightarrow C_5 \Leftrightarrow C_4 \Leftrightarrow C_3 \Leftrightarrow O_1 \Leftrightarrow B_2$$

Scheme I

TABLE III

Most Likely Fit of Scheme II to Four TPrA Concentrations

Rate constant	Value	Rate constant	Value
k_{12}	16.4	k_{54}	2610
k_{13}	4105	k_{56}	579.6
k_{21}	10762	k_{65}	199.2
k_{31}	36977	k_{67}	43.04
k_{34}	4913	k_{76}	117.7
k_{43}	2126	k_{78}	1.864
k_{45}	8701	k_{87}	9.123

Units of the rate constants are s^{-1} except for k_{12} which is $\times 10^6\ M^{-1}\ s^{-1}$. The values of the four TPrA concentrations are 0, 100, 500, 1,000 μM.

where the open, closed, and blocked kinetic states are represented by *O*, *C*, and *B*, respectively. The rate constant from any state C_i to state C_j may be represented as k_{ij} (refer to Table III). Scheme I was fit to control and three TPrA concentrations simultaneously (McManus and Magleby, 1991) and the most likely rate constants are shown in Table III. In this kinetic model, only the rate constant k_{12} was affected by blocker concentration. All other rate constants were independent of TPrA concentration. Thus, the blocker binds only to the open kinetic state and the channel cannot close with the blocker still bound. Alternative mechanisms were explored, such as adding blocking transitions to one or more closed states, but none of these mechanisms were more likely than the simple exclusive open state model. The rate constants generated by fitting this kinetic scheme to the data (Table III) are consistent with those calculated from Tables I and II, above.

QA Size Affects Unblocking Rate

All three of the QAs produced qualitatively similar effects on the open and closed interval distributions as did TPrA. The distributions of open and closed interval durations for one patch under control conditions and in the presence of TPrA (250 μM), TBA (500 μM), and TPeA (500 μM) are presented in Fig. 8. The time constants and relative areas for maximum likelihood fits of sums of exponentials to this data are shown in Tables IV and V. The time constants of the open states were decreased from 0.67 ms to ~0.1−0.2 ms by the blockers. Only a single open kinetic state could be distinguished under control conditions and in the presence of all of the blockers except for TPeA at the recording bandwidth of 6.2 kHz, while two open states were barely significant in the presence of TPeA. Both of the open components in the presence of TPeA exhibit nearly the same time constant and for the following analysis we have lumped them together (τ = 0.12 ms).

In the four experiments that could be analyzed in detail, the value of the open time constant usually decreased in the order: control, TPrA, TBA, and TPeA, although there was no significant difference between the reduction in open state time constants. The major effect of these QAs on the closed interval distribution was to add a closed interval component whose time constant increased as a func-

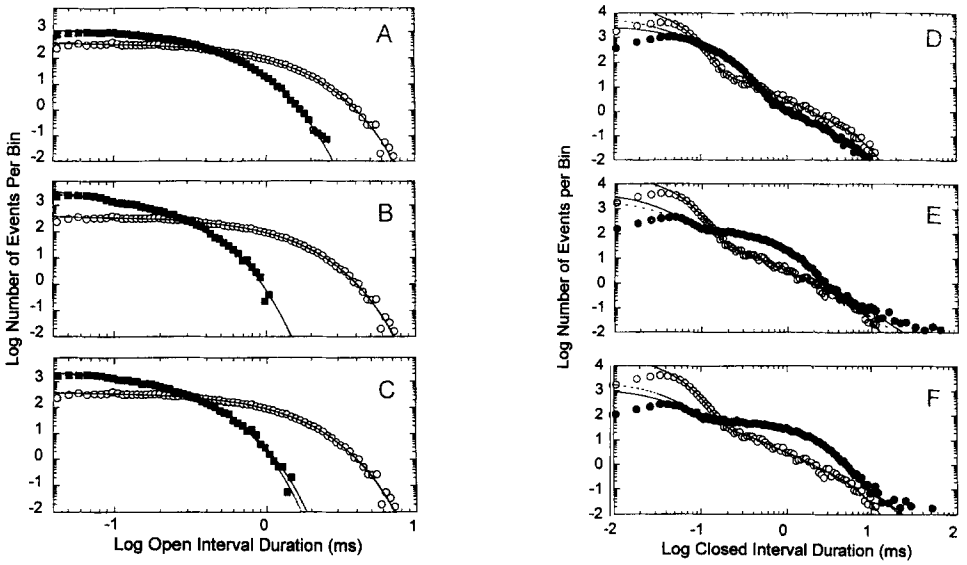

FIGURE 8. Open and closed dwell-time distributions from a single membrane patch containing one fast Cl channel under control conditions (*open circles*), and in the presence of 250 μM TPrA (*A* and *D*); 500 μM TBA (*B* and *E*); and 500 μM TPeA (*C* and *F*). For illustrative purposes only every fourth data point was plotted. Distributions were normalized such that they all represent the same number of events as under control conditions (open, 909,000; closed, 9,760). Solid lines represent the most likely set of exponential time constants and relative areas and the dotted lines (which superimpose on the solid lines except for longer times in *C* for TPeA, and for shorter times in *D-F*) represent the most likely set of rate constants for Scheme II, all of which were constrained to control values except for the unblocking (k_{21}) rate constant that was freely variable. Another set of solid lines, which represent the most likely rate constants of the unconstrained Scheme II (values for blocking and unblocking rates in Table VI), is present that exactly superimpose over the exponential fits.

tion of the size and hydrophobicity of the QA. This phenomenon is apparent in the closed interval distributions of Fig. 8 as a hump in the distributions that occurs at longer durations as the QA size is increased.

With no QA present, 97% of the intervals originate from the most brief closed exponential component with a time constant of ~25 μs. The remainder of the intervals originated from exponential components of longer duration with time constants of from 0.2–2.5 ms (for this analysis only those closed interval durations between 0.1 and 10 ms were used), each giving rise to <1% of these longer closed intervals. In the presence of 500 μM TPrA, the relative contribution of the briefest exponential component was reduced to 27% and a new component with a time constant of ~90 μs appeared that comprised 73% of the intervals. This 90-μs closed interval component gave rise to the broad hump apparent in the closed interval distribution in the presence of TPrA. Likewise, in the presence of the longer chain QAs TBA and TPeA, the closed interval distributions were dominated by an exponential component not present in the control distributions. For TBA this component had a time constant of ~0.45 ms and gave rise to 29% of the intervals, while

TABLE IV

Distribution of Open Interval Durations in the Presence of QA's

Control		TPrA		TBA		TPeA	
τ	area	τ	area	τ	area	τ	area
0.67	1.0	0.24	1.0	0.12	1.0	0.12	1.0

Time constants (τ) in ms and fractional areas represent the most likely parameters for the sums of exponential components that describe the distributions of open interval durations in the presence of 250 μM TPrA, 500 μM TBA, and 500 μM TPeA, for one patch. Membrane potential is −47 mV. Bandwidth is 6.2 kHz. All open intervals with durations between 0.1 ms and 10 ms were used for these distributions. The likelihood ratio test was used ($p < 0.10$) to determine the number of exponential components required to best fit each dwell-time distribution. At the $p < 0.05$ level, the findings are the same except that the TPeA distribution has two components with τ's of 0.11 and 0.16 ms and fractional areas of 0.42 and 0.58, respectively.

for TPeA, the component had a time constant of ~1 ms, and gave rise to 79% of the closed interval durations. Since the magnitudes of these increased components were so small, some of the components present under control conditions could not be resolved in the presence of blockers.

Again, the rate constants for blocking and unblocking were calculated from the time constants in Tables IV and V. K_s for blocking were 10.7×10^6 M^{-1} s^{-1}, 13.7×10^6 M^{-1} s^{-1}, and 15.2×10^6 M^{-1} s^{-1} and k_s for unblocking were 11,494 s^{-1}, 2,273 s^{-1}, and 917 s^{-1} for TPrA, TBA, and TPeA, respectively.

Q-Matrix Fitting to Obtain Rate Constants for QA Kinetic Scheme

Because the longer closed intervals were not affected by QAs (refer to Tables II and V), we have used a truncated kinetic model incorporating only the four closed states of briefest mean lifetime, a single open state, and a blocked state:

$$C_6 \Leftrightarrow C_5 \Leftrightarrow C_4 \Leftrightarrow C_3 \Leftrightarrow O_1 \Leftrightarrow B_2$$

Scheme II

where the open, closed, and blocked kinetic states are represented by *O*, *C*, and *B*, respectively. The rate constant from any state C_i to state C_j may be represented as k_{ij} (refer to Table VI). The use of this simplified scheme should not detract from any of our conclusions, as the closed states longer than those used in this analysis are variable and are composed of a very small number of events. Additionally, we have analyzed a limited number of records with six or seven closed states and find no consistent effect of any of the QAs on the rate constants between these long-lived states.

Table VI presents the most likely blocking (k_{12}) and unblocking (k_{21}) rate constants and the dissociation constant (K_d) for the simplified model when all 10 rate constants were completely unconstrained. The ability of this model to fit the data was also examined under conditions where all of the rate constants except the blocking and unblocking rate constants were constrained to the best fit values obtained under control conditions. The values for k_{12} and k_{21} for the constrained fits

TABLE V

Distribution of Closed Interval Durations in the Presence of QA's

	Compound							
	Control		TPrA		TBA		TpeA	
n	τ	A	τ	A	τ	A	τ	A
1	0.026	0.97	0.030	0.24	0.017	0.67	0.042	0.14
2	0.24	0.02	0.087	0.73	0.44	0.29	1.09	0.79
3	0.88	0.007	0.33	0.02	1.02	0.03	3.1	0.07
4	2.68	0.005	1.35	0.01	5.80	0.01	—	—
5	—	—	6.25	0.00		—	—	—

For legend see Table IV.

The values of the QA concentrations are as follows in micromolar: 250 TPrA, 500 TBA, 500 TPeA.

were within 10% of the values reported in Table VI, although the likelihoods of the constrained models were significantly less than those for the unconstrained models. Even though the likelihoods of the constrained fits were less than those of the unconstrained fits, the constrained models provided an excellent fit to the experimental open and closed interval distributions. The dashed lines in Fig. 8, which nearly superimpose over the exponential fits are the predictions of the constrained model with two unconstrained parameters.

The rate constants generated by fitting this kinetic scheme to the data (Table VI) are consistent with those calculated from Tables IV and V.

DISCUSSION

Using single-channel records, we have shown that TPrA, TBA, and TPeA block the fast Cl channel. The block is resolvable in open and closed time histograms as an additional closed state. The lifetime of the blocked state is dependent on the QA blocker, with larger QAs having slower unbinding rates and longer lifetime blocked states. All the QAs tested blocked the open state of channel activity and resulted in a reduced lifetime for the open state. Kinetic schemes with QA binding only the open state accurately fit the experimental data.

TABLE VI

Blocking, Unblocking, and Dissociation Constants for Scheme I

	Compound		
Rate constant	TPrA	TBA	TPeA
k_{12} ($\times 10^6\ M^{-1}\ s^{-1}$)	19.5 ± 6	13.0 ± 4	12.5 ± 2.5
k_{21} (s^{-1})	12896 ± 2381	2326 ± 220	1024 ± 87
K_d (k_{21}/k_{12}) (M)	661×10^{-6}	180×10^{-6}	82×10^{-6}

Values represent mean ± standard error for the results from three separate membrane patches.

Similarities between Fast Cl Channel and K Channel Block

Many of the properties of fast Cl channel block by TEA and derivatives are similar to those of K channel block as measured at the level of single channels. For example, Villarroel, Alvarez, Oberhauser, and Latorre (1988) and Carl, Frey, Sanders, and Kenyon (1993) reported that for large conductance Ca-activated K channels from skeletal muscle or turtle colon, block by intracellular TEA exhibited rapid kinetics while block by more hydrophobic TEA derivatives exhibited much slower kinetics. Using a more indirect method than used in the present study, Villarroel et al. (1993) reported K_ds for the block of BK channels in lipid bilayers by internal QAs of (in millimolar): 34, 17, and 0.5 for TEA, TPrA, and TBA, respectively. These values are in the same order and of similar magnitude as the values of 12, 0.66, and 0.18 mM for TEA, TPrA, and TBA found by us in this and a previous study (Sanchez and Blatz, 1992). Carl et al. (1993) also found that the larger and more hydrophobic TPeA had a much lower K_d than did TEA applied internally. A similar enhancement of block by larger and more hydrophobic QAs was found by Kirsch, Taglialatela, and Brown (1991) for cloned RCK2 K channels expressed in *Xenopus* oocytes. For these channels, however, the block observed in the presence of TPeA exhibited an extremely slow unblocking rate of 5×10^{-6} s^{-1} resulting in periods of normal channel activity with long silent (blocked) periods superimposed. Thus, it appears that the internal QA binding site of neuronal fast Cl channels is remarkably similar to that of large conductance, Ca-activated K channels. A major difference between BK channel and fast Cl channel QA block is the dependence of BK channel block on membrane potential. Intracellular TEA block of fast Cl channels is not voltage dependent (Sanchez and Blatz, 1994) and preliminary experiments have not been able to demonstrate any voltage dependence for internal block by the larger QAs, but this may be due to complications of the large concentration gradients used.

Larger and More Hydrophobic QAs Bind More Tightly to Blocking Site

Block of fast Cl channels by TEA is manifested as an apparent reduction in single-channel conductance, accompanied by subtle changes in gating kinetics that are consistent with very rapid binding and unbinding (Sanchez and Blatz, 1992). The lifetimes of the open and blocked states in the presence of TEA are so brief that the observed openings are actually composed of many openings and blockages that are attenuated to a level of reduced conductance by the required electronic filtering of the data record. In contrast, the larger and more hydrophobic symmetric derivatives of TEA, such as TPrA, TBA, and TPeA induce blocked states that have much longer lifetimes and are therefore well resolved as brief closing events during open intervals. The overall effect is a reduction in the true mean open interval duration and the appearance of a new component in the distribution of closed intervals. The mean lifetime of this new closed distribution component is relatively independent of the blocker concentration but is highly sensitive to the particular blocking compound with the smaller TPrA inducing a blocked component with a lifetime of ~90 μs that increased to over 1 ms in the presence of the larger, more hydrophobic TPeA. This finding suggests that there must be a hydrophobic region surround-

ing or near the QA binding site, as has been suggested for the QA binding site of K channels (Armstrong, 1971; French and Shoukimas, 1981; Swenson, 1981; Villarroel et al., 1988). Interactions between the more hydrophobic QAs and this site must stabilize the binding, resulting in a slower off-rate and consequent longer mean blocked lifetime.

All QAs Bind Preferentially to Open Kinetic States

The most obvious effect of QA block of fast Cl channels is the reduction of mean open duration. The fact that the simple kinetic mechanism of Scheme 1, with QAs binding solely to the open state, is sufficient to account for all of the blocking properties of the QAs suggests that the channel must enter the open state for block to occur. Although these observations do not rule out binding to closed states, they argue strongly that, if binding to closed states occurs, it does not lead to channel block, nor does it affect channel gating in any way.

This work was supported by National Institutes of Health grants HL-07360 and NS-30584.

Original version received 8 June 1994 and accepted version received 15 May 1995.

REFERENCES

Armstrong, C. M. 1971. Interaction of tetraethylammonium ion derivatives with the potassium channels of giant axons. *Journal of General Physiology.* 58:413–437.

Armstrong, C. M. 1975. Ionic pores, gates, and gating currents. *Quarterly Review of Biophysics.* 7:179–210.

Barrett, J. N., K. L. Magleby, and B. S. Pallotta. 1982. Properties of single calcium-activated potassium channels in cultured rat muscle. *Journal of Physiology.* 331:211–230.

Blatz, A. L. 1991. Properties of single fast chloride channels from rat cerebral cortex neurons. *Journal of Physiology.* 441:1–21.

Blatz, A. L., and K. L. Magleby. 1986*a*. Correcting single channel data for missed events. *Biophysical Journal.* 49:967–980.

Blatz, A. L., and K. L. Magleby. 1986*b*. Quantitative description of three modes of activity of fast chloride channels from rat skeletal muscle. *Journal of Physiology.* 378:141–174.

Blatz, A. L., and K. L. Magleby. 1989. Adjacent interval analysis distinguishes among gating mechanisms for the fast chloride channel from rat skeletal muscle. *Journal of Physiology.* 410:561–585.

Carl, A., B. W. Frey, S. M. Ward, K. M. Sanders, and J. L. Kenyon. 1993. Inhibition of slow-wave repolarization and Ca-activated K channels by Quaternary ammonium ions. *American Journal of Physiology (Cell Physiology).* 264:C625–C631.

Choi, K. L,. C. Mossman, J. Abue, and G. Yellen. 1993. The internal quaternary ammonium receptor site of *Shaker* potassium channels. *Neuron.* 10:553–541.

Colquhoun, D., and F. J. Sigworth. 1983. Fitting and statistical analysis of single-channel records. In Single Channel Recording. B. Sakmann and E. Neher, editors. Plenum Publishing Corp., NY. 191–264.

Colquhoun, D., and A. G. Hawkes. 1983. The principles of stochastic interpretation of ion-channel mechanisms. *In* Single Channel Recording. B. Sakmann and E. Neher, editors. Plenum Publishing Corp., New York. 135–176.

French, R. J., and J. J. Shoukimas. 1981. Blockade of squid axon potassium conductance by internal tetra-n-alkylammonium ions of various sizes. *Biophysical Journal.* 34:271–291.

Hamill, O. P., A. Marty, E. Neher, B. Sakmann, and F. J. Sigworth. 1981. Improved patch-clamp techniques for high-resolution current recording from cells and cell-free membrane patches. *Pfügers Archiv.* 391:85–100.

Hartmann, H. A., G. E. Kirsch, J. A. Drewe, M. Taglialatela, R. H. Joho, and A. M. Brown. 1991. Exchange of conduction pathways between two related K channels. *Science.* 251:942–944.

Hille, B. 1992. Ionic Channels of Excitable Membranes, 2nd ed. Sinauer Associates, Inc., Sunderland, MA. 605 pp.

Horn, R., and K. Lange. 1983. Estimating kinetic constants from single channel data. *Biophysical Journal.* 43:207–223.

Kay, A. R., and R. K. S. Wong. 1986. Isolation of neurons suitable for patch-clamping from adult mammalian central nervous system. *Journal of Neuroscience Methods.* 16:227–238.

Kirsch, G. E., M. Taglialatela, and A. M. Brown. 1991. Internal and external TEA block in single cloned K channels. *American Journal of Physiology (Cell Physiology).* 261:C583–C590.

MacKinnon, R., and G. Yellen. 1990. Mutations affecting TEA blockage and ion permeation in voltage-activated K channels. *Science.* 250:276–279.

McManus, O. B., and K. L. Magleby. 1991. Accounting for the Ca-dependent kinetics of single large-conductance Ca-activated K channels in rat skeletal muscle. *Journal of Physiology.* 443:739–777.

McManus, O. B., A. L. Blatz, and K. L. Magleby. 1987. Sampling, log binning, fitting, and plotting durations of open and shut intervals from single channels and the effects of noise. *Pfügers Archiv.* 410: 530–553.

Rao, C. R. 1973. Linear statistical inference and its applications. John Wiley & Sons, Inc., NY. 625 pp.

Sanchez, D. Y., and A. L. Blatz. 1992. Voltage-dependent block of fast chloride channels from rat cortical neurons by external tetraethylammonium ion. *Journal of General Physiology.* 100:217–231.

Sanchez, D. Y., and A. L. Blatz. 1994. Block of neuronal fast chloride channels by internal tetraethylammonium ions. *Journal of General Physiology.* 104:173–190.

Stanfield, P. R. 1983. Tetraethylammonium ions and the potassium permeability of excitable cells. *Review of Physiology, Biochemistry, and Pharmacology.* 91:1–67.

Swenson, R. P., Jr. 1981. Inactivation of potassium currents in squid axons by a variety of quaternary ammonium ions. *Journal of General Physiology.* 77:255–271.

Villarroel, A., O. Alvarez, A. Oberhauser, and R. Latorre. 1988. Probing a Ca-activated K channel with quaternary ammonium ions. *Pfügers Archiv.* 413:118–126.

Weiss, D. S., and D. L. Magleby. 1990. Voltage dependence and stability of the gating kinetics of the fast chloride channel from rat skeletal muscle. *Journal of Physiology.* 426:145–176.

Yellen, G., M. Jurman, T. Abramson, and R. MacKinnon. 1991. Mutations affecting internal TEA blockade identify the probable pore-forming region of a K channel. *Science.* 251:939–941.